The *Salvinia* Paradox: Superhydrophobic Surfaces with Hydrophilic Pins for Air Retention Under Water

By *Wilhelm Barthlott,* Thomas Schimmel,* Sabine Wiersch, Kerstin Koch, Martin Brede,* Matthias Barczewski, Stefan Walheim, Aaron Weis, Anke Kaltenmaier, Alfred Leder,* and *Holger F. Bohn*

Superhydrophobic surfaces are of high scientific and economic interest because of their remarkable properties.[1–3] However, the best and most efficient surfaces known so far evolved in plants (e.g. Lotus) and animals.[4–6] Whereas superhydrophobicity and self-cleaning are well explored in biological and technical surfaces,[7] little attention was given to their air-retaining properties under water. Air-retaining surfaces are of great technological, economic and ecological interest, e.g., for low friction fluid transport and drag reducing ship coatings.[8,9] Here, we show the sophisticated surface design of the floating water fern *Salvinia* offering a novel mechanism for long-term air-retention. The hierarchical architecture of the leaf surface is dominated by complex elastic eggbeater-shaped hairs coated with nanoscopic wax crystals. But, surprisingly, the terminal cells of each hair lack the wax crystals and form evenly distributed hydrophilic patches, covering about 2% of the otherwise completely superhydrophobic leaf surface. We demonstrate that these hydrophilic patches stabilize the air layer by pinning the air–water interface to the tips of the eggbeater hairs. This prevents the loss of air caused by formation and detachment of gas bubbles due to instabilities especially in a turbulent flow environment. The unique combination of hydrophilic patches on superhydrophobic surfaces (''Salvinia Effect'') provides a promising concept for the development of a coating with long-term air-retention properties.

In millions of years optimized superhydrophobic surfaces have evolved in plants and animals, which now serve as models for the development of biomimetic materials. The classic example is the self-cleaning surface of the Lotus leaf (*Nelumbo nucifera*). Caused by the hierarchically structured surface of the leaves consisting of microstructured pappilose cells superimposed by a nanostructure of hydrophobic wax crystals water forms almost perfect spheres (''fakir droplets'').[4,10–12] Droplets are in the so called Cassie State, sitting on top of the microstructure with air pockets remaining between leaf surface and water.[13] Submerged in water these surfaces show a silvery reflection, resulting from air trapped between the microstructures.[14–16] Such air films significantly reduce the shear stress and thus the surface friction drag of these surfaces.[17] Especially in microfluidic systems research the use of drag reducing superhydrophobic surfaces is currently en vogue.[18–20] But also for long distance transport of fluids and even for ship hulls with reduced friction the usage of air-retaining surfaces is discussed. Even though high drag reduction of up to 50% was measured using micro- or nanostructured technical superhydrophobic surfaces, an effect recently called ''giant liquid slip'', the practicality is tempered by the short time (few minutes) the air films persisted.[21–25]

However, several plant and animal species exist, which possess complex structured surfaces capable of holding an air film under water for a long time (days to months).[26,27] These air films fulfill various purposes, ranging from respiration to insulation. Plant and animal species living on the water surface evolved air-retaining surfaces to prevent wetting and submersion. Here we focus on the floating water fern *Salvinia molesta*, well known for its incredible rapid dispersal power and the ecological problems caused.[28]

The upper side of the floating leaves of *S. molesta* is densely covered with complex multicellular hairs (Fig. 1a). Four hairs are grouped together and elevated on a large emergence, leading to structures with a total height of about 2 mm (Fig. 1b). The terminal ends of the four hairs are connected, forming an eggbeater-shaped structure. In adult leaves the terminal cell of each hair is collapsed, forming a cap of four dead cells (Fig. 1c). With exception of these four cells the whole leaf is covered with wax crystals (Fig. 1d). As a result the surface of the terminal cells is rather smooth, whereas the wax crystals create a nanoscale roughness on all other cells (Fig. 1d). We found almost identical hair structures in *S. biloba* and *S. auriculata*.[29]

[*] Prof. W. Barthlott, S. Wiersch, Dr. H. F. Bohn
Nees-Institut für Biodiversität der Pflanzen
Rheinische Friedrich-Wilhelms-Universität
Meckenheimer Allee 170, 53115 Bonn (Germany)
E-mail: barthlott@uni-bonn.de
Prof. Th. Schimmel, Dr. M. Barczewski, Dr. S. Walheim, A. Weis, A. Kaltenmaier
Institute of Applied Physics and Center for Functional Nanostructures (CFN)
University of Karlsruhe
Karlsruhe Institute of Technology (KIT)
76131 Karlsruhe (Germany)
Institute of Nanotechnology and Center for Functional Nanostructures (CFN)
Forschungszentrum Karlsruhe
Karlsruhe Institute of Technology (KIT)
76021 Karlsruhe (Germany)
E-mail: thomas.schimmel@physik.uni-karlsruhe.de
Prof. K. Koch
Biologie und Nanobiotechnologie
Hochschule Rhein-Waal
Landwehr 4, 47533 Kleve (Germany)
Dr. M. Brede, Prof. A. Leder
Lehrstuhl Strömungsmechanik
Fakultät für Maschinenbau und Schiffstechnik
Universität Rostock
Albert-Einstein-Straße 2, 18059 Rostock (Germany)
E-mail: martin.brede@uni-rostock.de

DOI: 10.1002/adma.200904411

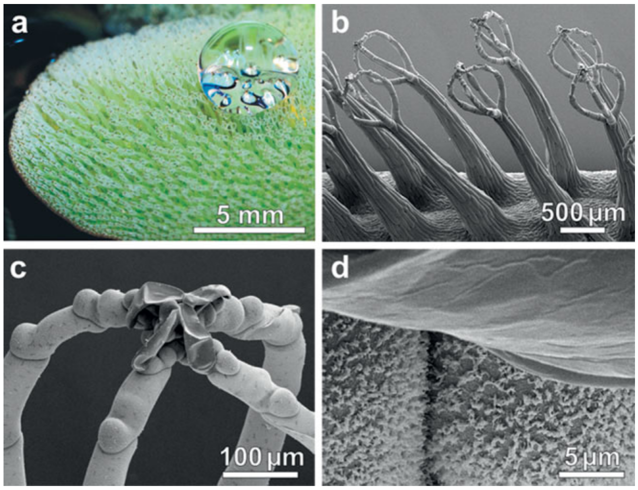

Figure 1. a–d) Morphology of *Salvinia molesta* floating leaf. a) Upper side of the leaf surface densely covered with hairs. The spherical shape of the water drop on the leaf indicates the superhydrophobic character of the surface. b–d) SEM images of the complex hair structures. b) Four multicellular hairs grouped on top of an emergence and connected at the terminal end leading to an eggbeater-shaped structure. c) The terminal cell of each hair is collapsed forming a patch of four dead cells. d) The whole leaf surface is covered with nanoscale wax crystals (below) with exception of the terminal cells (above).

Submerged in water the leaves are capable of holding an air layer for several weeks presumably limited by the lifetime of the leaves. When emerging to the surface the water skin rips and the dry leaf appears without any sign of surface wetting. Individual water drops form round spheres, showing the strong hydrophobicity of the surface (Fig. 1a). Larger drops roll off the surface at the slightest tilting or vibration. Surprisingly when pulling a small droplet across the leaf surface, the tips of the eggbeater hairs stick to the droplet forming a meniscus. The adhesion is so strong that the elastic hairs bend and swing back when the tips snap off the droplet. This indicates that the tips of the hair structures become easily wetted by water.

To test this, we froze fresh *S. molesta* leaves covered with droplets of a water-glycerol solution and observed the contact zone using low-temperature scanning electron microscopy (SEM) (Fig. 2a). The lateral view revealed that the terminal cells were wetted by the solution (Fig. 2b,c). The shape of the meniscus between the droplet and the terminal cells indicates a good wettability of the cell surface.

To identify distribution and size of these wettable areas we submerged fresh *S. molesta* leaves in distilled water stained with 0.01% methylene blue. Light microscopy studies showed that the terminal cells of each eggbeater structure were stained dark (Fig. 3). This indicates that only these minute "hydrophilic patches", i.e., small areas with significantly increased wettability, become wetted while on the remaining hydrophobic parts of the leaf surface the staining solution rests on the tips of the wax crystals. Analysis of ten methylene blue stained *S. molesta* leaves produced a mean value of 233 ± 29 hydrophilic patches per square centimeter covering $2.2\% \pm 0.9\%$ of the whole area. In *S. biloba* an almost identical area ($2.2\% \pm 0.4\%$) is formed by 322 ± 22 smaller hydrophilic patches per square centimeter.

To investigate the properties of the air–water interface in vivo, we directly imaged the interface on top of submerged leaves of

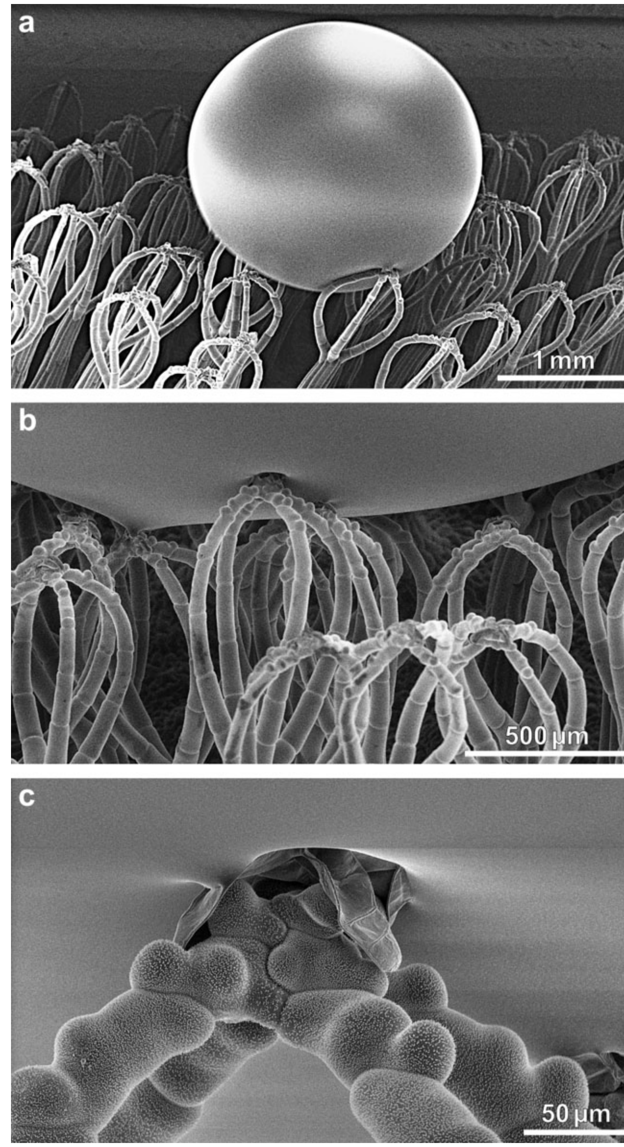

Figure 2. Low-temperature SEM of a frozen leaf with applied droplet of a water–glycerol solution (a). Lateral view of the contact zone showing a hydrophilic meniscus between the water–glycerol droplet and the terminal cells (b, c).

S. molesta and *S. biloba* in situ by multi-focus optical microscopy. From the microscopy images the morphology of the interface is clearly visible (Fig. 3b). Figure 3b shows that the eggbeater shaped structures very efficiently act as pillars supporting the air–water interface (tent-like), preventing it from further approaching the leaf surface. The depressions of the air–water interface observed between supporting pillars are governed by the Young–Laplace equation, where the shape of the interface is determined by the air-layer pressure and water pressure as well as the liquid–solid contact angle.[30]

The hydrophilic patches at the tips of the hairs presumably stabilize the air film against pressure fluctuations (see below). First experimental results using a microscopic device for the observation of the flow[31] show that the air–water interface is subject to considerable oscillations while the leaf is exposed to

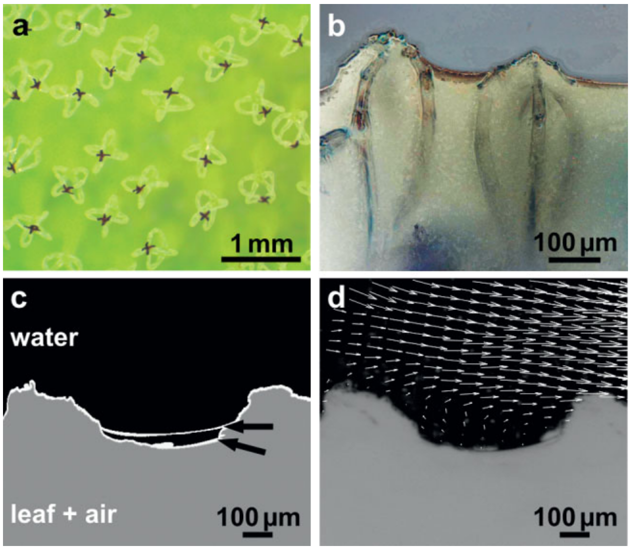

Figure 3. Characteristics of the air–water interface. a) Optical microscopy image of the leaf surface after submersion in 0.01% methylene blue solution. Hydrophilic areas were stained in dark. b) Optical microscopy image of the air–water interface on a submersed leaf of *S. molesta*. The interface rests on top of the eggbeater structures. c) Overlay of the air–water interface lines (white) from four instantaneous images of a *Salvinia* leaf with air layer (grey) subjected to a tangential, steady fluid flow (black) with a velocity of 0.6 ms^{-1}. d) Micro-particle image velocimetry measurement of the instantaneous velocity vector field on a *Salvinia* leaf with recirculation between the hairs. Velocity of the oncoming flow was 0.6 ms^{-1}.

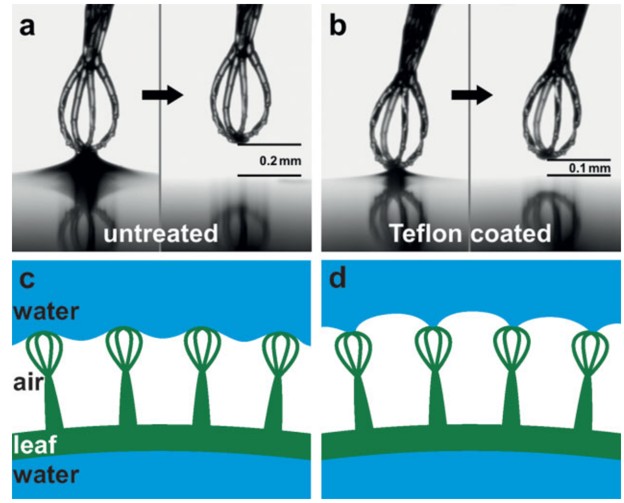

Figure 4. Meniscus-pulling experiment with an untreated (a) and Teflon-coated (b) *S. molesta* hair. The tip of the untreated hair (a) is hydrophilic, leading to a stronger pinning to the water surface compared to the Teflon coated hair (b). The distance between the hair tip and water surface at the exact instant when the meniscus snapped off is shown. c,d) Schematic of the air retention by a submerged *Salvinia* leaf (green). Both hydrophobic repulsion (c) and pinning by the attractive hydrophilic tips of the hairs (d) stabilize the air–water interface.

tangential water flow of 0.6 ms^{-1}. Experimentally obtained air–water interface lines from different time steps depicted in Figure 3c demonstrate that the interface is spanned between the hairs, but its distance to the leaf base is variable due to oscillations. The hydrophilic patches pin the air–water interface to the tips of the eggbeater structures and thus prevent partial lift-off and air loss due to the oscillations. As a secondary effect, the wetting of the terminal cells is also causing zero velocity conditions at the surface of the wetted area, subsequently inducing flow separation at the tips of the hairs. An example for a flow separation and the forming of a recirculating flow region is presented in Figure 3d, obtained using 2D micro-particle image velocimetry (μPIV). As a result of the flow separation the average tangential velocity directly on the air–water interface in between the hairs is reduced. Thus the risk of volume loss from the air film due to the oscillations process is minimized.

To demonstrate the pinning effect, individual eggbeater hairs were dipped into water. From a lateral view the shape and size of the water meniscus created, when pulling the hairs out of the water was recorded (Fig. 4a,b). As a measure of the hydrophilicity we took the distance between the tip of the hairs and the water surface at the exact instant when the meniscus snapped off. This experiment was done with untreated hairs and hairs that were rendered hydrophobic by dipping them into a Teflon (polytetrafluoroethylene, PTFE) solution. The water meniscus could be pulled roughly twice as high by the untreated hair (0.2 mm, Fig. 4a) than by the Teflon coated hair (0.1 mm, Fig. 4b).

The function of the eggbeater hairs is obvious – they allow the trapping of a thin air layer reaching from the surface of the plant leaf to the top of the hairs. Penetration of water into this well-defined region requires energy for creating an increased contact area between the water and the hydrophobic hairs.

This also explains the special eggbeater shape of the structures. In order to stabilize the air–water interface most efficiently, it is desirable that the energy required for the water to penetrate into the region between the hairs is maximized. Therefore it makes sense that the hairs are split into four arms to create as much surface per height difference as possible.

To enhance this effect even more, these four arms are bent together at the terminal ends, approaching an almost horizontal angle. This leads to a maximization of the additional water-hair contact area per height difference required for the water to penetrate into the air retention area, i.e., to penetrate deeper than the topmost level of the hairs.

At this point, the question arises what the function of the hydrophilic patches at the tips of the otherwise completely hydrophobic eggbeater hairs might be. It is obvious that they do not contribute to the stabilization of the air–water interface against penetration closer towards the plant leaf which we described above (Fig. 4c). On the other hand it is also obvious that if the air–water interface moves further apart from the leaf than the level given by the top of the eggbeater hairs (Fig. 4d), this also costs energy because breaking the contact between the hydrophilic patches needs an activation energy.

Delamination of the water layer will thus take place in a two-step process:

(i) When the air–water interface is pulled apart from the plant leaf by external forces (surge), the water will initially continue to be pinned at the hydrophilic patches (Fig. 4d) and only the air–water interface *between* neighboring patches will be withdrawn from the equilibrium level defined by the top end of the hairs. Energy will be needed for this deformation, which results in an increase of the air–water interface.

(ii) Only after a threshold value of the force per area pulling at the air–water interface is exceeded, the contact between the hydrophilic patches and the water will finally be disrupted and the air–water interface is no longer pinned to the hydrophilic patches at the top of the eggbeater hairs.

To conclude the unique combination of hydrophilic patches on an otherwise superhydrophobic surface serves one common purpose: the stabilization of the air–water interface at a predefined level at the top of the hairs. A deviation from this level costs energy in both directions. When the air–water interface approaches the plant surface, energy is needed for the wetting of the hydrophobic hair surface, whereas when the air–water interface moves further apart from the plant surface, energy is needed for increasing the interface area and finally for breaking the contact between the hydrophilic patches and the water.

To prevent this rupture of contact, the elastic properties of the eggbeater hairs obviously are advantageous. They allow for a small deformation of the air–water interface in both directions, and the elastic mechanical forces of the deformed hairs, which approximately can be described by Hooke's Law, help to restore the equilibrium position of the air–water interface relative to the surface of the leaf.

In this way, the air–water interface is stabilized against oscillations of this interface in space and time. The advantage of this stabilization for the plant is obvious: typically, such oscillations lead to a loss of air by formation of small bubbles if the air–water interface moves too far away from the plant surface. Local currents and local and temporal pressure fluctuations are common in running water and for moving objects, and these fluctuations finally lead to a rapid loss of the air film on the surface. The pinning of the air–water interface at hydrophilic patches significantly increases the activation energy needed for the formation of air bubbles.

The limited progress in the development of technical air-retaining surfaces almost solely stems from their limited capability to keep the air layer for longer times and under rough conditions typically occurring in turbulent flows.[21,22] It appears that the ''Salvinia Effect'', i.e., pinning of the air–water interface at a predefined level by hydrophilic patches, is a key for solving this problem. It opens intriguing perspectives for designing artificial surfaces on the basis of this effect with long-term air-retaining properties – for a wide range of applications from drag reducing ship coatings and low-friction fluid transport to novel concepts for thermally insulating interfaces.

Experimental

Morphological Analysis: Critical-point-dried *Salvinia* leaves were investigated using standard scanning electron microscopy (SEM) procedures. For examination of the contact zone fresh leaves with drops of a water-glycerol solution were frozen and observed using low-temperature SEM.

Multi-focus Imaging: For enhanced depth of field images of the air–water interface leaves of *S. molesta* were cut and submerged in water. The section of the cut was then multi-focus imaged with a standard light microscope with an immersion objective (10×).

Flow Measurements: *Salvinia* leaves were placed in a closed loop micro channel and exposed to a steady, tangential flow of water with seeding particles. Micro-particle image velocimetry (μPIV) was then performed using a pulsed light source for a volume illumination of the flow region, microscopic imaging of the seeding particles in the focal plane with a double frame CCD camera and a cross correlation analysis of the images [32].

Meniscus-Pulling Experiment: Tips of *S. molesta* hairs were hydrophobized by coating with Teflon AF (Dupont) solved in FC77 (3M). Coated and uncoated individual *S. molesta* hairs were fixed to a linear stepper motor and gradually submerged in water and pulled out again. This was monitored with a CCD camera. Immediately after the snap-off of the water meniscus the distance between the tip of the hair and the water surface was measured.

Acknowledgements

We are indebted for financial support of the work by the German Federal Ministry of Education and Research (BMBF), the German Research Foundation (DFG), and the Landesstiftung Baden-Württemberg within the Network of Excellence ''Functional Nanostructures''. We thank Roland Gröger (Karlsruhe) and Hans-Jürgen Ensikat (Bonn) for their support.

Received: December 23, 2009
Published online: April 28, 2010

[1] R. Blossey, *Nat. Mater.* **2003**, *2*, 301.
[2] M. Callies, D. Quéré, *Soft Matter* **2005**, *1*, 55.
[3] P. Roach, N. J. Shirtcliffe, M. I. Newton, *Soft Matter* **2008**, *4*, 224.
[4] W. Barthlott, C. Neinhuis, *Planta* **1997**, *202*, 1.
[5] T. Wagner, C. Neinhuis, W. Barthlott, *Acta Zool.* **1996**, *77*, 213.
[6] K. Koch, W. Barthlott, *Phil. Trans. R. Soc. A* **2009**, *367*, 1487.
[7] A. Solga, Z. Cerman, B. F. Striffler, M. Spaeth, W. Barthlott, *Bioinspir. Biomim.* **2007**, *2*, 1.
[8] J. J. Corbett, H. W. Koehler, *J. Geophys. Res.* **2003**, *108*, 4650.
[9] V. Eyring, H. W. Köhler, J. van Aardenne, A. Lauer, *J. Geophys. Res.* **2005**, *110*, 17305.
[10] W. Barthlott, in *Application of the Scanning EM in Taxonomy and Functional Morphology* (Ed: D. Claugher,), Clarendon Press, Oxford **1990**, 69.
[11] D. Quéré, *Nat. Mater.* **2002**, *1*, 14.
[12] K. Koch, B. Bhushan, W. Barthlott, *Soft Matter* **2008**, *4*, 1943.
[13] A. B. D. Cassie, S. Baxter, *Trans. Faraday Soc.* **1944**, *40*, 546.
[14] R. E. Johnson, R. H. Dettre, *Adv. Chem. Ser.* **1964**, *43*, 112.
[15] S. Herminghaus, *Europhys. Lett.* **2000**, *52*, 165.
[16] A. Marmur, *Langmuir* **2006**, *22*, 1400.
[17] J. Kim, C.-J. Kim, *Proc. IEEE MEMS 2002*, **2002**, 479.
[18] J. Ou, B. Perot, J. P. Rothstein, *Phys. Fluids* **2004**, *16*, 4635.
[19] N. Nguyen, S. Wereley, *Fundamentals and Applications of Microfluidics*, Artech House, London **2006**.
[20] F. Feuillebois, M. Z. Bazant, O. I. Vinogradova, *Phys. Rev. Lett.* **2009**, *102*, 026001.
[21] A. K. Balasubramanian, A. C. Miller, O. K. Rediniotis, *AIAA J.* **2004**, *42*, 411.
[22] C. Henoch, T. N. Krupenkin, P. Kolodner, J. A. Taylor, M. S. Hodes, A. M. Lyons, K. Breuer, *3rd AIAA Flow Control Conf*, San Francisco, CA, **2006**.
[23] C.-H. Choi, C.-J. Kim, *Phys. Rev. Lett.* **2006**, *96*, 4.
[24] C. Lee, C.-J. Kim, *Langmuir* **2009**, *25*, 12812.
[25] Y. C. Jung, B. Bhushan, *J. Phys. Condens. Matter* **2010**.
[26] Z. Cerman, B. F. Striffler, W. Barthlott, in *Functional Surfaces in Biology: Little Structures with Big Effects*, Vol. *1* (Ed: S. N. Gorb,), Springer, Berlin **2009**.
[27] C. W. Heckman, *Int. Rev. Gesamten Hydrobiol. Hydrogr.* **1983**, *68*, 715.
[28] P. A. Thomas, P. M. Room, *Nature* **1986**, *320*, 581.
[29] W. Barthlott, S. Wiersch, Z. Čolić, K. Koch, *Botany* **2009**, *87*, 830.
[30] W. Konrad, C. Apeltauer, J. Frauendiener, W. Barthlott, A. Roth-Nebelsick, *J. Bionic Eng.* **2009**, *6*, 350.
[31] M. Brede, M. Witte, A. Leder, *13th Intl. Symp. Appl. Laser Techniques to Fluid Mechanics*, Lisbon, Portugal **2006**.
[32] R. J. Adrian, *Annu. Rev. Fluid Mech.* **1991**, *23*, 261.